A HIGH PERFORMANCE 50 KW THREE-PHASE PFC POWER SUPPLY FOR USE WITH A DC ARC PLASMA TORCH

Jean-Paul Dubut, Alexandre Magnus Fernandes Guimarães,
Andrés Ortiz Salazar*, André Laurindo Maitelli*, Clodomiro Alves Júnior**

Instituto Nacional de Pesquisas Espaciais - INPE
Centro Regional de Natal e Fortaleza - CRN
Av. Salgado Filho, nº 3000
Caixa Postal 130
59001-970 - Natal – RN – Brazil
Phone: +55842314733 – Fax: +55842314941
jean@crn.inpe.br, alexandre@crn.inpe.br

Universidade Federal do Rio Grande do Norte - UFRN
DEE/DCA*/DFTE**
Campus Universitário, s/nº
59072-970 - Natal – RN – Brazil
Phone: +55842153696 – Fax: +55842513767
andres@dca.ufrn.br, maitelli@dca.ufrn.br,
alvesjr@dfte.ufrn.br

***Abstract* - This paper describes the concept, the project and the practical construction of a 50 kW three-phase boost PFC power supply for supplying a non-transferred DC arc plasma torch used in a waste treatment plant. This PFC power supply is endowed of three independent circuits for power factor correction to attempt the power factor and current harmonic level IEC 61000-3-4 standard. The PFC preregulator stage uses the average current-mode control implemented by a PWM control scheme. The power stage is built on an industrial IGBT three-phase bridge rectifier module configured in a boost rectifier topology that supplies the 800V_{DC} output voltage. ZCT soft switching techniques were implemented to minimize the rectifier structure commutation losses. A dedicated microcontroller unit executes the supervision, the task management, the running sequence and the main programming parameters as well as the protection function of the associated subsystems. Using an external microcomputer, a RS-232 serial input allows the remote programming of the PFC power supply, the plasma torch and reactor supervisory, and the overall industrial process control. Simulations in PSpice were implemented to aid the definition of the boost rectifier topology and predict the results. All experimental tests were realized over a 50 kW programmable resistive load. This paper highlights the PWM boost rectifier, the PFC preregulator and the compensator loop circuit design.**

KEYWORDS

Power factor correction, three-phase boost rectifier, ZCT soft switching, PWM power supply, plasma torch.

I. INTRODUCTION

In order to have this work context well situated and to understand the proposed development importance of this project, it is necessary to remind the recent exigencies imposed by the environmental legislation, national agencies of regulation (CONAM, ANVISA, etc.) and other federal, state and municipal inspection orgs demanding the industrial and medical sector to provide the adequate treatment and an appropriate destination for the produced waste. Due to the processing, storage and discard high costs produced by the new environmental exigencies, it is important to considerate the aggregated value to the waste. The non-organic components can be recycled or vitrified, and the organic parts can be dissociated in order to generate synthesis gases, thermal and/or electrical energy in co-generation scheme.

The waste treatment plant, experimentally operated by the DFTE/UFRN department, seeks to demonstrate the potential of plasma technology [1] and its new application fields, especially to the hospital and radioactive waste treatment.

The described three-phase PFC power supply is destined to have an equipped experimental waste treatment plant using the thermal plasma techniques to destroy industrial waste. A three-phase PFC power supply, a non-transferred DC arc plasma torch, a process reactor and its associated auxiliary systems essentially constitute the main elements plant. This project intends to offer a significant contribution to the research line on electrical power conversion systems, held by the automation and control systems area of the UFRN-PPgEE. Also, it represents an effort to attempt the university-industry integration program [2], by offering effective local solutions for the industrial park demand.

The figure 1 presents the illustrative diagram of the experimental waste treatment plant, the three-phase PFC power supply and its several associated peripheral systems.

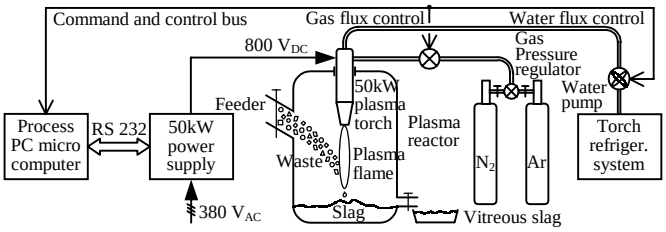

Fig. 1 - Illustrative diagram of the waste treatment plant and the associated PFC power supply

The PFC power supply specification was done for supplying a 50kW DC arc plasma torch leading a 0.5m^3 internal volume reactor using a pyrolysis process. The project attempts to the IEC 61000-3-2 and IEC 61000-3-4 standards for a current harmonic level rejection in the utility line. The emphasis given to the article is willfully descriptive in order to facilitate the general understanding of the plasma waste treatment system and the purpose of its associated PFC power supply.

II. PROJECT DESCRIPTION

For the project specification of the PFC power supply and its associated subsystems [3], the following items were considered as being of major importance and for this reason they were implemented in the system:

a) To provide the galvanic isolation between the utility line and the DC output PFC power supply for eliminating any voltage leakage possibilities, feedback current and operator electrocution risks during the plant operation;
b) To assure the automatic and continuous adjustment of the power factor near the unity and to maintain the harmonic current level and spurious under the limit imposed by the IEC 61000 standards;
c) To assure the control and adjustment of the PFC power supply parameters in the standalone mode;
d) To include an automatic protection and alarm to protect the PFC power supply, the DC arc plasma torch, the cooling pump, the plasma reactor, the flow gas regulator and any associated equipment, signaling to the operator;
e) To detect and automatically suppress the DC arc discharge between the plasma torch electrodes, plasma reactor body and metallic waste under treatment;
f) To remotely program and control the electrical parameters of the PFC power supply by an auxiliary process PC microcomputer through the RS-232 serial communication port;
g) To present good functional modularity of the units in order to allow easy "in situ" maintenance, as well as to permit the system evolution in the future.

The figure 2 presents the simplified PFC power supply block diagram and its associated subsystems.

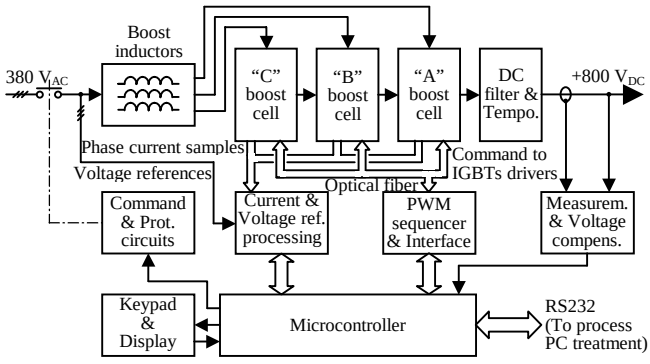

Fig. 2 – Simplified block diagram of the three-phase PFC power supply and associated subsystems

To attempt the electrical specifications and general requests, the six-pulse PWM boost rectifier topology [4] was chosen as being the most appropriate configuration for this application.

A 75kW external transformer provides the galvanic isolation between the plant utility line and the three-phase PFC power supply output connected to the DC arc plasma torch. The primary welding of this three-phase isolation transformer is connected in a Δ scheme and the secondary welding in a Y scheme. The adopted Δ/Y configuration permits the free circulation of the third harmonic due to the magnetizing current in the primary phases and generates a neutral reference for the auxiliary circuits [5]. The primary-to-secondary winding ratio is made 1:0,58. The utility line-to-line nominal voltage at the transformer primary input is $380V_{AC}$ and the phase-to-phase nominal voltage at the transformer secondary is $380V_{AC}$. The secondary voltage is applied to the input PWM boost rectifier.

A SEMIKRON SFM84-50/4 three-phase low-pass filter is inserted between the secondary windings of the isolation transformer and the PWM boost rectifier input in order to reduce harmonic currents injection and spurious produced by the 20kHz rectifier IGBT switching.

Three LEM LA-50S magneto-resistive sensors measure the PWM boost rectifier three-phase currents. These current samples are used for the power factor correction of the PFC power supply after they have been rectified, amplified and processed. Additionally, they are also used for the PWM boost rectifier over-current protection.

Two 3VA SEMIKRON SMT3/1 auxiliary small transformers, connected between phases and neutral point, generate the current references for phases A and B. In order to guarantee the total current equilibrium condition $I_A+I_B+I_C=0$, the phase C current reference is generated by the vectorial sum of the phases A and B. This is obtained by means of an electronic adder and represents the necessary condition for an independent phase power factor correction.

Three 1mH boost inductors are constructed on iron-siliceous laminated C core presenting a magnetic area core of $35cm^2$. The coil is distributed on two legs of the core in order to minimize the magnetic dispersion and uses paired wiring windings. Each inductor presents a two-3mm air gap. The boost inductor stores a 2J energy and weights about 20kg.

The main boost rectifier is built on a SEMIKRON SKM145GB123D [6] IGBTs three-phase bridge rectifier module including an internal anti-parallel diode. These devices offer a 150A/1200V commutation current capability and they are mounted on an extruded aluminum heat sink with air forced cooling. The ZCT soft switching auxiliary circuit is built on a SEMIKRON SKM75GB123D IGBTs three-phase bridge module including an internal anti-parallel diode. These devices offer a 75A/1200V commutation current capability and they are also mounted on a main extruded aluminum heat sink. Three LC resonant tanks are connected between each arm of the main rectifier and auxiliary ZCT leg, working as a snubber. The resonant tank is designed to make the peak resonant current I_{pk} exceed the instantaneous maximal boost inductor current [7] in order to achieve ZCT operation. A good compromise design is obtained to fix I_{pk} current about 1.25 times of the maximal switching phase current and the resonant period is chosen as 4μs to guarantee safe operation. A 4μH L_{na} inductor and 0.5μF C_{na} capacitor constitute each resonant tank circuit leg. Six SEMIKRON SKH22H4 dual-driver modules drive the main and auxiliary IGBT devices. These modules also provide the electrical interface between the PWM command unit and the IGBT three-phase bridges. Each dual-driver module incorporates the over-voltage and over-current protection circuits to protect its IGBT pair.

The PWM three-phase rectifier permits the output voltage adjustment from $+700V_{DC}$ to $+900V_{DC}$ under any load condition. It offers sufficient regulation margin to comply a ±15% utility line voltage variation.

The figure 3 presents the simplified electrical diagram of the PWM boost rectifier structure.

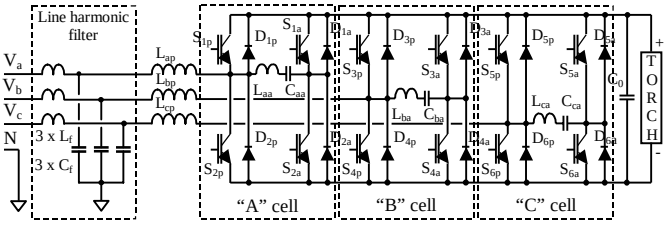

Fig. 3 – Simplified electrical diagram of the PWM boost rectifier

In order to simplify the IGBT PWM command, the implemented strategy control does not permit the energy reverse flux from the load to the source. This condition was assumed because the PFC power supply does not operate with regenerative load.

The PWM generator unit is built on three UNITRODE UC3854B dedicated PFC preregulator devices [8]. These integrated circuits, using an associated logic, generate the complementary PWM signals to command the IGBT main switches, the complementary signals to command the IGBT ZCT auxiliary switches and implement the control strategy. Each phase current is synthesized from a reference generated by the corresponding phase. The control loop commands the PWM that force the line current in phase with the line voltage, with a displacement factor near to zero. In this way, the harmonic generation is minimized and it is possible to suit the power factor near the unity. Additionally, the UNITRODE UC3854B implements the current and voltage protection functions, duty-cycle limiting or disabling the IGBT PWM pulses.

A 4N25 optocoupler and its associated circuit are used to sampling and interfacing the output PWM rectifier to the compensator in order to maintain the output voltage to the adjusted level. The compensator range is enough to maintain stable the output voltage in despite of the utility line and load variations.

The output DC voltage of the boost rectifier is filtered and stored by a double bank of three 4700μF/450V_{DC} electrolytic capacitors connected to a serial scheme. This capacitor bank was dimensioned in order to maintain the ripple voltage at the 1% specified value under any load condition. At the PFC power supply starting the high current charge of the electrolytic capacitor bank is limited by a 2.2Ω/500W serial power resistor. After some seconds, a temporized contactor short-circuits this resistor and the total rectified voltage is applied to the capacitor bank.

The microcontroller unit, based on a FREEDOM 16 commercial board manufactured by INTEC AUTOMATION INC, performs the PFC power supply command and supervision. This O&M board uses a MOTOROLA 68HC16Z1 microprocessor and offers some 10 bit A/D input ports, 12 bit D/A output ports, two PWM output ports, some bi-directional I/O ports, keypad interface and a two lines 64 character LCD output. Also, it offers both RS-232 and RS-485 I/O serial ports. The microcontroller unit is programmed in micro C language and provides a debug compilation port. This unit allows to set the PFC power supply operating parameters such as output voltage and output current applied to the DC arc plasma torch. In standalone mode, the parameters programming is performed by its associated keypad and the assumed values are displayed on a LCD. In the remote mode, the parameters programming is realized by means of a RS-232 serial port under control of the process PC microcomputer. Additionally, the microcontroller unit activates the alarms and signalizes to the plant operator, from the programmed limit values.

The command and protection unit implements the running sequence, the low starting and the general protection of the PFC power supply. Several electromechanical contactors commanded by a logical circuit board essentially constitute this unit. A diazed fuse set protects the utility line input and complements the protection of the PFC power supply.

III. POWER FACTOR CORRECTION PREREGULATOR TOPOLOGY

The boost rectifier operates in the continuous mode conduction and an independent power factor correction was implemented, one for each phase, acting in a current mode control. In a way to simplify the necessary functions, UNITRODE UC3854B [9] integrated circuits were used, one for each phase of the rectifier structure.

The figure 4 presents the simplified block diagram of the UC3854B PFC preregulator circuit [10] used in each phase of the PWM boost rectifier.

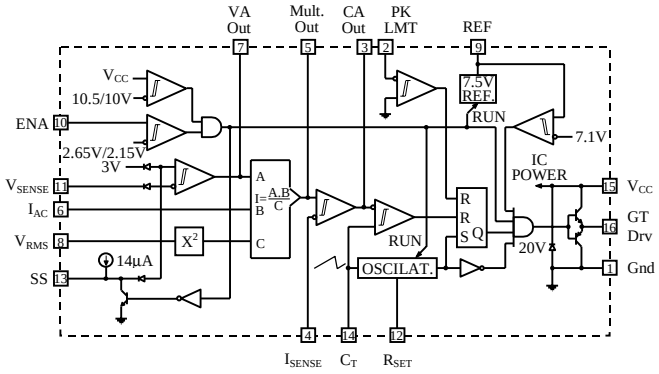

Fig. 4 - Simplified block diagram of the UC3854B PFC preregulator circuit

These devices incorporate the analog multiplier, the voltage references, the current and voltage comparators, the PWM oscillator and some amplifiers to generate and control the PWM signal. The PWM signal to command the IGBTs switches is generated at the fixed 20kHz nominal frequency and the three devices are synchronized for minimizing the harmonic beat between the phases. These signals are addressed to the IGBT driver modules by means of an associated logic that implements the PWM boost rectifier command strategy. The sequential command of the boost rectifier element switching defined by a sinusoidal modulation law forces the phase current envelope to be in phase with the input phase voltage reference, presenting a null displacement. By a permanent comparison between the current phase sample and the current reference, it is possible to synthesize the phase current at the boost rectifier input, reducing the harmonics and, for this way, resulting in a high power factor near the unity.

As mentioned in the previous paragraph, the C phase current is synthesized to the virtual reference generated by the vectorial sum of phase A and B references. This artifice is used to guarantee the equilibrium condition for the input phase currents in the PWM boost rectifier.

IV. PWM BOOST RECTIFIER, ZCT CIRCUIT AND COMPENSATORS PROJECT

The PWM rectifier power stage to be controlled is composed by three independent boost structures as shown in figure 3. The used method for the project system specifies a small signal model and each functional block is represented by its transference function. The diagram presented in figure 5 illustrates the small signal model and the several system transference function blocks.

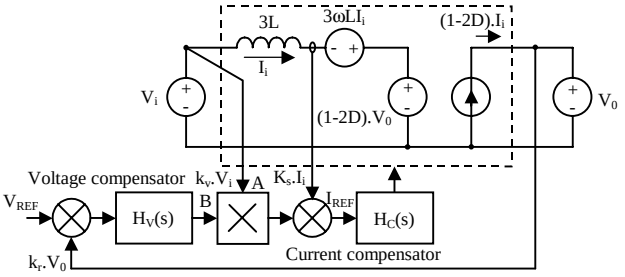

Fig. 5 – Diagram of the PFC rectifier small signal model

4.1 Power stage design:

The transference characteristic [11] between the input voltage, V_i, applied on each boost circuit and the output voltage, V_0, is defined by the equation:

$$\frac{V_0}{V_i} = \frac{2}{1-(2 \cdot D_n)} \quad (1)$$

The previous equation (1) can be rewritten in terms of the effective conduction time, t_c, related to period switching T_s. Then:

$$t_c = \left[\frac{1}{2} - \frac{V_i}{V_0}\right] \cdot T_s \quad (2)$$

If considered the phase A, the voltage applied to inductor is equal to V_i and defined by:

$$V_i \cdot \sin(\theta) = L \cdot \frac{\Delta I}{\Delta t} \quad (3)$$

The maximum inductor voltage V_L occurs for $\theta = 90°$. Therefore, it is necessary to determine when the maximum Δt occurs, resulting in a maximum current ripple [12]. Due to sinewave symmetry it is sufficient to analyze the interval between 0° to 90º. Applying the phase voltage equations and after some mathematical manipulation:

- For the interval between 0° and 30°, where $V_B<V_A<V_C$:

$$L_n = \sin(\theta) \cdot \left[1 + \frac{V_i}{V_0} \cdot [\sin(\theta - 120°) - \sin(\theta - 240°)]\right] \quad (4)$$

Where L_n can be called the normalized inductance and is defined by:

$$L_n = \frac{L \cdot \Delta I}{T_s \cdot V_i} \quad (5)$$

- For the interval between 30° and 90°, where $V_B<V_C<V_A$:

$$L_n = \sin(\theta) \cdot \left[1 + \frac{V_i}{V_0} \cdot [\sin(\theta - 120°) - \sin(\theta)]\right] \quad (6)$$

Since the ripple voltage in phase A is maximum at 90°, then:

$$L = \frac{\left(1 - 1.5 \cdot \frac{V_i}{V_0}\right) \cdot V_i}{\Delta I \cdot f_s} \quad (7)$$

The maximum value of the input current is determined in function of the output power, rectifier efficiency, input voltage and number of the boost circuit arms that supply power to the load.

$$I_{RMS} = \frac{P_0}{3 \cdot \eta \cdot V_{RMS}} \quad (8)$$

The maximum current at 60Hz component that will flow through the inductors is given by:

$$I_{pk} = I_{RMS} \cdot \sqrt{2} \quad (9)$$

A good compromise between the current ripple and the peak current is to allow 10% ripple to average ratio. Then:

$$\Delta I_L = 0.1 \cdot I_{pk} \quad (10)$$

The value of the output capacitor effects both hold-up time and output voltage ripple. Choosing the ripple criteria, where V_{0R} = 1%, the following equation will give a value for C_0:

$$V_{0r} = 0.01 \cdot V_0 \quad (11)$$

$$C_0 = \frac{P_0}{2 \cdot \pi \cdot 360 \cdot V_0 \cdot V_{0R}} \quad (12)$$

The ZCT L_{na} and C_{na} resonant elements values for the chosen T_0 period are defined as:

$$T_0 = 2 \cdot \pi \cdot \sqrt{L_{na} \cdot C_{na}} \quad (13)$$

$$Z_0 = \sqrt{\frac{L_{na}}{C_{na}}} \quad (14)$$

$$I_{pk} = \frac{V_0}{Z_0} \quad (15)$$

4.2 Control loops design

In order to simplify the control loops design it is used the small signal model PFC boost converter. All functional blocks needed to implement the PFC boost rectifier functions as the PWM modulator, the comparator, the multiplier, the current and voltage compensators are provided by the UNITRODE UC3854B integrated circuit.

4.2.1 Current loop design:

This design uses the average current mode control loop. A LEM LA50S magneto-resistive sensor furnishes the measured input phase current sample. For design simplification, it is considerate the virtual voltage, V_{RSH}, produced on the equivalent resistance R_{SH}; the comparator output voltage, V_{CEA}, and the saw oscillator output voltage, V_s. Then, a transfer function may be expressed in terms of the comparator output voltage and the oscillator output voltage. Thus:

$$G_C(s) = \frac{V_{RSH}}{V_{CEA}} = \frac{V_0 \cdot R_{SH}}{s \cdot L \cdot V_s} \quad (16)$$

The design of the average current mode control loop begins with choosing a crossover frequency. The switching frequency, f_s, of the PWM boost rectifier is 20kHz chosen and the compensator loop dimensioning should take into account the sampling effect of the transfer function represented by the equation:

$$H_S(s) = 1 - \frac{s}{2 \cdot f_s} + \left(\frac{s}{\pi \cdot f_s} \right)^2 \quad (17)$$

The current compensator bandwidth must be sufficiently large in order to guarantee that the phase current follows the reference signal. As the current reference is a rectified sinusoidal, it is observed that after the 15th harmonics being 900Hz, the superior order components do not offer significant contribution and they cause a small degradation in the power factor. On the other hand, the current compensator criteria design suggested by UNITRODE are the following:

a) To locate the zero compensator at least one decade of the switching frequency f_s in order to obtain a fast response and good tracking of the reference current signal;
b) To locate the pole compensator not more than half of the switching frequency f_s in order to reduce the ripple at the frequency switching;
c) To define the current compensator gain in the flat bandwidth at least 10dB in order to obtain a secure margin phase;
d) To define the open loop frequency transfer function crossing about ¼ of the switching frequency.

In this specific design, the crossover frequency, f_c, was fixed to 7.5kHz. The transfer function for the UNITRODE UC3854B current compensator is represented by:

$$H_c(s) = \frac{-(1 + s \cdot C_z \cdot R_z)}{s \cdot R_i (C_z + C_p) \cdot \left[1 + s \cdot \left(\frac{C_z \cdot C_p}{C_z + C_p} \right) \cdot R_z \right]} \quad (18)$$

In this way, the transfer function of the open loop current $TFOL_c$ is represented by:

$$TFOL_c(s) = G(s) \cdot H_c(s) \cdot H_S(s) \quad (19)$$

Substituting the transfer function terms in the previous equation (19), then:

$$TFOL_c(s) = \left(\frac{V_0 \cdot R_{SH}}{V_s \cdot s \cdot L} \right) \cdot \left[\frac{1 + s \cdot C_z \cdot R_z}{s \cdot R_i (C_z + C_p) \cdot \left[1 + s \cdot \left(\frac{C_z \cdot C_p}{C_z + C_p} \right) \cdot R_z \right]} \right] \cdot \left[1 - \frac{s}{2 \cdot f_s} + \left(\frac{s}{\pi \cdot f_s} \right)^2 \right] \quad (20)$$

After some mathematical manipulation using Matlab and regarding to the established criteria, then:

a) Compensator loop gain:

$$H_C = \frac{1}{G_C} = \frac{1}{\left(\frac{V_0 \cdot R_{SH}}{V_s \cdot s \cdot L} \right)} = \frac{R_z}{R_i} \quad (21)$$

b) Zero frequency compensator loop:

$$f_z = \frac{f_s}{10} = \frac{1}{2 \cdot \pi \cdot R_z \cdot C_z} \quad (22)$$

c) Pole frequency compensator loop:

$$f_p = \frac{f_s}{2} = \frac{1}{2 \cdot \pi \cdot R_z} \cdot \left(\frac{C_z + C_p}{C_z \cdot C_p} \right) \quad (23)$$

4.2.2 Voltage loop design

For design the voltage loop it is necessary to determine the amount of ripple on the output voltage. In order to meet the 5% THD IEC 61000 standard specification, the distortion due to output ripple voltage feeding through the voltage error amplifier must be limited to 1%. This allows 1,5% distortion from the multiplier and some distortion originated from other sources. To obtain a low distortion THD and a high power factor it is necessary that the input phase current tracks the reference voltage sample and the output voltage variations. The voltage loop design however will be attempt two antagonist criteria. At first, the bandwidth must be sufficiently large in order to present a good response for the transients. In second place, to present a slow loop voltage response in order to no modulate the reference signal through the ripple voltage. A low-pass filter meets a compromise with a bandwidth fixed at ¼ of the ripple frequency.

The power stage gain $G_V(s)$ of the converter can be expressed in terms of P_{IN}, V_0, C_0 and ΔV_{VEA}. It is given by:

$$G_V(s) = \frac{P_0}{3 \cdot \Delta V_{VEA} \cdot V_0 \cdot s \cdot C_0} \quad (24)$$

The voltage compensator transfer function is presented by the equation:

$$H_V(s) = \frac{V_{VEA}}{V_0} = \frac{-R_p}{R_i \cdot (1 + s \cdot C_p \cdot R_p)} \quad (25)$$

By the derivate and extract terms, thus

$$R_i \cdot C_p = \frac{10 \cdot V_{0R} \cdot V_{REF}}{2 \cdot \pi \cdot 360 \cdot V_0} \quad (26)$$

$$f_c = \frac{1}{2 \cdot \pi} \cdot \sqrt{\frac{P_0 \cdot V_{REF}}{3 \cdot V_0^2 \cdot V_{VEA} \cdot C_0 \cdot R_i \cdot C_p}} \quad (27)$$

$$R_p = \frac{1}{2 \cdot \pi \cdot f_c \cdot C_p} \quad (28)$$

4.3 Component values

Some PWM PFC rectifier components values are determinate by the previous related equations. The Table I synthesizes the input parameters and main components values.

TABLE I

PFC rectifier input parameters and component values

Input parameters	
V_{IN} = 220V phase to neutral or 380V phase to phase	P_0 = 50kW V_0 = 800V_{DC} $\Re$ = 1%
f_{IN} = 60Hz	R_0 = 62.5Ω
Rectifier components	
L_b = 1mH	r_{Lb} = 0.01Ω
L_{na} = 4μH	C_{an} = 0.5μF
C_0 = 3,300μF	r_{C0} = 0.02Ω
f_s = 20kHz	
Current compensator components (f_z = 1kHz; f_p = 7.5kHz; |H(s)| = 10dB)	
R_z = 27kΩ	C_z = 1.2nF
R_i = 4.7kΩ	C_p = 100pF
Voltage compensator components (f_c = 30Hz)	
R_p = 10kΩ	C_p = 330nF
R_i = 100kΩ	

V. RESULTS

The topology validation of the PFC power supply was obtained with aids of the PSpice and Matlab simulations. The following figures present the waveform simulations, as the experimental result measurements in phase A with a high

power dummy load. The results presented in phases B and C are similar.

The figure 6 presents an amplified view of the voltage and current waveforms in phase A around the passage by the zero axis obtained during the PSpice simulation circuit.

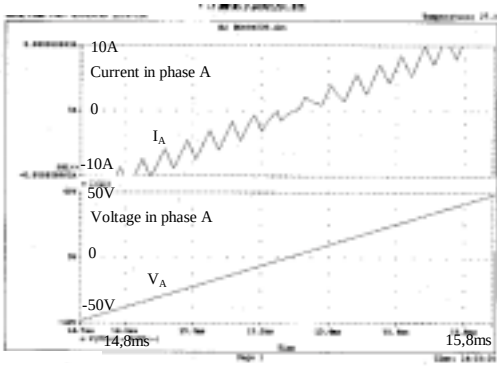

Fig. 6 – Amplified view of the current and voltage waveforms in phase A

The figure 7 shows the displacement factor waveforms between the voltage and current in phase A.

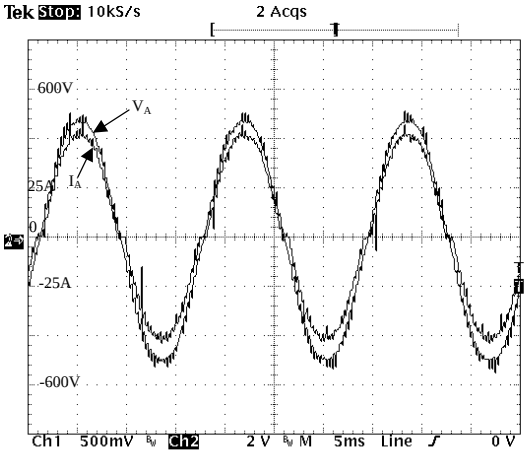

Fig. 7 - Voltage and current waveforms in phase A

The figure 8 shows the FFT current waveforms observed in phase A with and without the PFC active function.

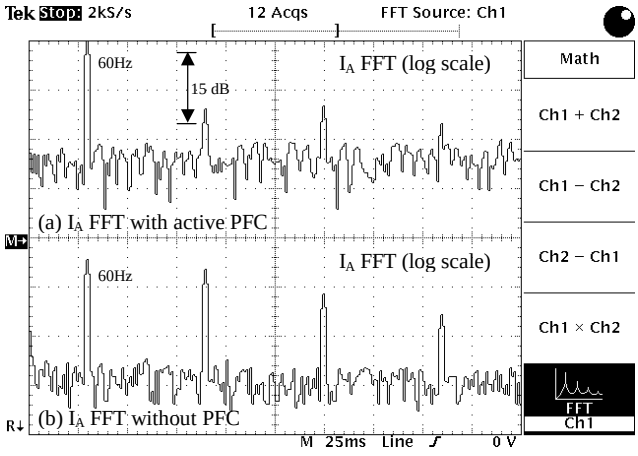

Fig. 8 - I_A current FFT observed in phase A: (a) with active PFC; (b) without PFC

When the PFC is active the current harmonic reduction observed in phase A is 15dB. Similar results are observed in phases B and C, thus the PFC is independent in each phase.

The global efficiency of the PFC power supply is nearly 93% at the 50kW nominal power and the total current harmonic distortion is inferior to 5%. The power factor obtained in each phase is 0,995 and the current harmonic content is quite low. All experimental tests were realized on a 50kW dummy load constructed for this application.

VI. CONCLUSIONS

Regarding to obtain results it is important to note that, in despite of its simplicity, the chosen PFC boost rectifier structure using the average current mode control and the ZCT soft switching implemented by the auxiliary circuit has presented good performance. The utilization of three independent power factor preregulator UNITRODE UC3854B integrated circuits simplified the control circuitry, requiring just an associated logic to generate the complementary commands for drive the IGBT switches.

The PFC power supply meets the IEC 61000 standards and allows its connection in the utility plant without introducing disturbances.

REFERENCES

[1] V. Dembovsky, “Plasma metallurgy”, Elsevier Science Publishing Company Inc., New York, N Y, USA, 1985.

[2] C. Alves Júnior, “Nitretação em plasma pulsado: equipamento, preparação e caracterização das camadas nitretadas”, Tese de Doutorado, UFSCar, Florianópolis, SC, Brasil, 1992.

[3] J. P. Dubut, “Uma proposta de fonte chaveada com correção do fator de potência para alimentação de um reator de nitretação iônica”, Dissertação de Mestrado, UFRN-CT-DEE, Natal, RN, Brasil, 2001.

[4] R. C. Souza and D. S. Simonetti, “Análise de operação de três topologias retificadoras trifásicas com pré-carga de corrente”, UFES-DEL-CT, Vitória, ES, Brasil, 1997.

[5] M. E. Fraser and C. D. Manning, “Four-wire power factor corrected boost rectifier”, EPE´95, Sevilla, Spain, 1995.

[6] SEMIKRON, “Semikron power electronics manual”, Nürnberg, Deutschland, 1998.

[7] J. Wu, H. Dai, K. Xing, F. C. Lee and D. Boroyevich, “Implementation of a ZCT soft switching technique in a 100kW PEBB based three-phase PFC rectifier”, VEPEC, Blacksburg, USA, 1999.

[8] Y. Jiang, H. Mao, F. C. Lee and D. Borojevic, “Simple high performance three-phase boost rectifiers”, VEPEC, USA, 1994.

[9] UNITRODE, “Power supply design seminar”, Merrimack, USA, 1995.

[10] UNITRODE, “High power factor preregulator”, Merrimack, USA, 1998.

[11] J. A. Pomílio, “Pré-reguladores de fator de potência - PFP”, UNICAMP-FEE, Campinas, SP, Brasil, 1997.

[12] A. R. Borges and A. J. Perin, “A high power factor current source rectifier with energy regeneration”, UFSC-DEE-INEP, Florianópolis, SC, Brazil, 1997.